


Article

Coral Tissue Regeneration and Growth Is Associated with the Presence of Stem-like Cells

Jonathan Levanoni ^{1,2,†}, Amalia Rosner ^{1,*}, Ziva Lapidot ¹, Guy Paz ¹ and Baruch Rinkevich ¹ 

¹ National Institute of Oceanography, Israel Oceanography and Limnological Research, Tel-Shikmona, P.O. Box 2336, Haifa 3102201, Israel; j.levanoni@gmail.com (J.L.); ziva@ocean.org.il (Z.L.); guy@ocean.org.il (G.P.); buki@ocean.org.il (B.R.)

² Department of Marine Biology, Leon H. Charney School of Marine Sciences, University of Haifa, P.O. Box 3338, Haifa 3498838, Israel

* Correspondence: amalia@ocean.org.il; Tel.: +972-48565233

† These authors contributed equally to this work.

Abstract: Members of the Cnidaria phylum were studied for centuries to depict the source of their unprecedented regeneration capacity. Although adult stem cells (ASCs) have been recognized in tissue growth/regeneration in many hydrozoans, there has not been any evidence of them in the ancestral Anthozoa class. This study sheds light on the development of epidermal epithelium expansion, akin to blastema, during tissue regeneration after small circular incisions (each 2.77 mm²) and during the natural expansion of tissue across a flat surface in the scleractinian coral *Stylophora pistillata*. Regeneration was completed within 9 days in 84.5% (n = 64) of the assays. About 35% of the samples regrew a single polyp, 60% showed no polyp regrowth, and approximately 6% exhibited multiple new polyps. We further used histological staining, pH3, Piwi immuno-histochemistry, and qPCR for eight stemness markers: *Piwi-1*, *Nanos-1*, *Nanos-1-like*, *Tudor-5*, *Tudor-7*, *Boule*, *Sox-2*, and *Myc-1*. The results revealed the formation of an “addendum”, an epidermal epithelium in the growing edges (in regenerating and normal-growing fronts) inhabited by a cluster of small cells featuring dense nuclei, resembling ASCs, many expressing pH3 as well as Piwi proteins. Most of the stemness genes tested were upregulated. These results indicate the participation of ASCs-like cells in tissue regeneration and growth in scleractinian corals.

Keywords: ASCs; Cnidaria; Anthozoa; coral; stem cell; *Stylophora pistillata*; tissue regeneration; wound healing; tissue growth; coral nubbins



Citation: Levanoni, J.; Rosner, A.; Lapidot, Z.; Paz, G.; Rinkevich, B. Coral Tissue Regeneration and Growth Is Associated with the Presence of Stem-like Cells. *J. Mar. Sci. Eng.* **2024**, *12*, 343. <https://doi.org/10.3390/jmse12020343>

Academic Editor: Azizur Rahman

Received: 29 December 2023

Revised: 9 February 2024

Accepted: 12 February 2024

Published: 17 February 2024



Copyright: © 2024 by the authors. Licensee MDPI, Basel, Switzerland. This article is an open access article distributed under the terms and conditions of the Creative Commons Attribution (CC BY) license (<https://creativecommons.org/licenses/by/4.0/>).

1. Introduction

As in other cnidarian taxa [1,2], one of the biological hallmarks of corals is their regeneration power, as coral colonies are capable of repairing lesions of various sizes, replacing lost tissues and polyps [3–5], and even regenerating the whole body (colony) from minute fragments [6,7]. These regenerative traits enable the colony to withstand a whole plethora of damages inflicted by physical and biological drivers, such as the result of (a) attacks by fish like parrotfish or pufferfish, which are capable of snipping off pieces of corals’ tissue and skeleton [8], (b) predation by invertebrates, such as snails and starfish, and corallivorous fish (e.g., butterflyfish), which consume just the coral tissue, leaving the skeleton intact [8,9], and (c) natural occurrences like storms and human-induced factors, such as touristic activities which can lead to mechanical damages such as colonial fragmentation [10–12] or tissue abrasion.

The ability of coral colonies to regenerate involves a demanding cascading process that necessitates the reconstruction of both the tissues and the skeletal structures, requiring the availability of both cells and energy resources [13–15] along with the proper machinery for pattern formation [16,17] of the regenerating structures. Ideally, the regeneration process should occur rapidly, as prolonged exposure of damaged tissue and exposed skeletons to

opportunistic turf organisms like invertebrates, algae, and bacteria can subject the colony to intense competition [18–21]. This underscores the urgent necessity for corals to quickly recover injured tissues and skeletal frameworks.

The regenerative power of scleractinian corals was first recognized over a century ago [22] and has since been the subject of extensive research. However, there is still limited knowledge regarding the cellular processes and the molecular machinery through which a colony regenerates lost tissues and polyps and heals wounds. Most studies conducted examinations on regeneration rates, rates by which denuded surface areas were recovered, and time periods for the complete repair of wounds at certain sizes [3–5,15,23–29]. Recent studies have delved into coral regeneration within the context of different environmental stress and conditions [30–32], aligning this with the physiological statuses of coral tissues [33,34]. Yet, there has not been a concentrated research focus on what are likely the essential components of coral regeneration, i.e., adult stem cells (ASCs), and their progenies.

Through the years, many indications for ASCs have been gathered within the phylum Cnidaria. The well-studied model organism for ASCs in cnidarians is the genus *Hydra* (Hydrozoa), where three lines of ASCs were identified: ectodermal, endodermal, and interstitial cells, or i-cells [35–39]. These different cell types act as precursors for various cell lineages and their descendants within their respective tissues, allowing for a remarkable regenerative power. In the Scyphozoa, there is evidence of the emergence of amoebocytes, which are hypothesized to fulfil a similar role to that of i-cells in hydrozoans [38,40–43]. These cells typically exhibit irregular shapes, and they are found in both epithelial tissues and mesoglea. It is suggested that they may move through filopodial extensions, allowing for their mobility within the organism. Yet, in the more primitive class of Anthozoa, there is limited evidence of the presence of ASCs. Most studies within this class have primarily identified amoebocytes in close vicinity to regenerating wounds, although their precise role in tissue regeneration remains a subject of debate [44–50]. It was suggested that their primary function may be the phagocytosis of various contaminants. Yet, another study [51] has revealed, for the first time in the Anthozoa, disorganized cell masses at the edges of growing tissues in nubbins of the branching coral *Stylophora pistillata*, a model species in the research on this topic [52]. The cells, located at the forefront of tissue growth, were described as small, round, and featuring prominent nuclei, characteristics typically associated with stem cells. Due to the scarcity of information on ASCs in corals, the remarkable repair and regeneration mechanisms in corals remain poorly understood. The cellular and molecular mechanisms governing these processes are entirely unknown.

This study seeks to explore the regeneration of wounds inflicted on 2D nubbin tissue of *S. pistillata*, examining both organismal and cellular levels, including dynamics, patterns, and rates. This research further compares the cellular and molecular mechanisms governing regeneration during wound healing, aiming to identify common factors in these processes and establish the central role of ASCs in *S. pistillata*'s regeneration. Additionally, we correlate well-established markers of ASCs with potential ASC candidates. The results affirm similar morphological patterns during regeneration and normal growth while revealing significant expression changes in common proliferation and stemness markers, highlighting the recruitment of ASC-like cells to active growth and regeneration sites, suggesting the potential involvement of ASCs in this coral's growth and regeneration.

2. Experimental Design and Methods

2.1. Collection and Maintenance

Three colonies of *S. pistillata* (permit restriction) that were naturally recruited and grew on the frames of a floating coral nursery, about 300 metres off the Northern Beach in Eilat, Israel (N 29° 32' 34.843" E 34° 58' 24.88"; 9–11 m depth), were tagged, collected, and translocated to the running water tables' facility at the Israel Oceanography and Limnological Research (IOLR, Haifa). The water tables are supplied with seawater pumped from the adjacent Mediterranean shoreline (about 1 m deep) and maintained under a

constant 24 °C temperature (using a chiller unit) and under a light regime of 12:12 h (light–dark), using metal halide spotlights (400 W, 10,000 K, and 14,000 K) [53].

2.2. Fragmentation and Lateral Growth

Following an acclimation period of at least two weeks, the coral colonies were fragmented into small nubbins, each constituted of at least ten polyps, using either wire cutters or a diamond-plated band saw (for the thicker parts of the colony), as described in [54], for the production of ca. 160 nubbins per colony. The employment of a nubbin assay allowed for the creation of a substantial number of repetitions for this research, with the ease of maintenance under laboratory conditions. The 2D-flattened tissues had additional advantages in studying wounds regeneration, as it is technically easier to inflict wounds on 2D tissues and locate and document changes during regeneration.

Then, the nubbins were attached to glass slides (two per slide) using Loctite superglue, fastening the nubbin's bare skeleton side to the glass [54]. The slides were inserted, four in each proprietary plastic rack placed into 20-L aquaria (similar conditions to the water tables). The nubbins were left to grow laterally on the substrates, as described in [51,54], and encrusted the slides until the tissue extended by at least 1 cm from the nubbin's base and a skeleton was formed underneath the expanded tissue (Figures 1 and 2(a1,a2)). The slides were cleaned with a sharp blade once a week to remove debris, algae, and pests.

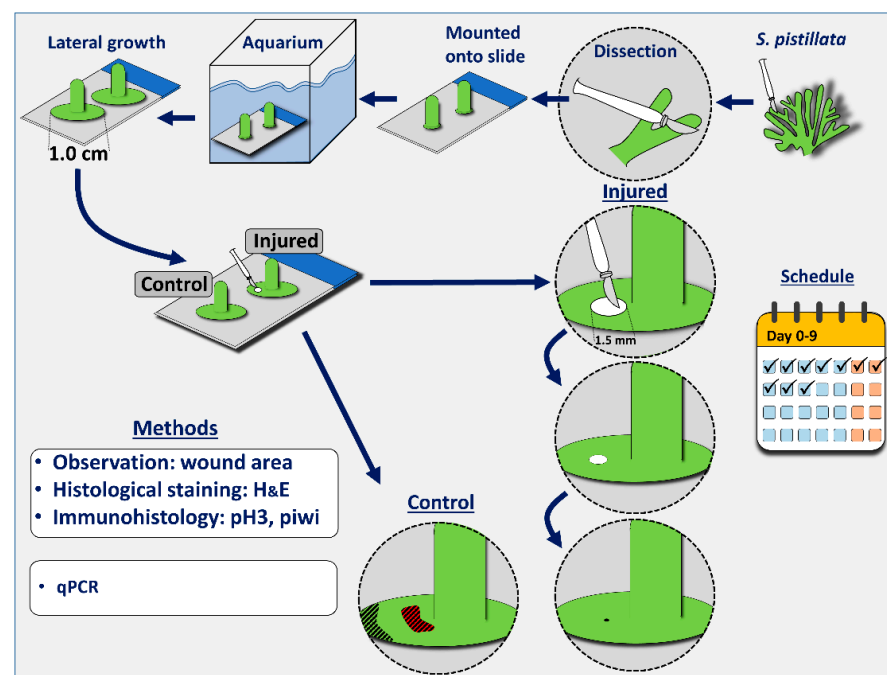


Figure 1. A schematic flowchart for the performed experiments. Following laboratory acclimatization, three *S. pistillata* coral genotypes were fragmented into nubbins (34 nubbins/genotype), which were affixed, two nubbins per glass slide. The nubbins were maintained in aquaria until the developed 2D-flattened tissues reached 1 cm in diameter, then injuries were inflicted by removing entire polyps from the centres of the tissues (30 nubbins/genotype) using a dermal punch, ensuring wound size homogeneity. The remaining nubbins served as the controls. Analyses performed: (1) Daily observations/quantifications on regeneration processes for 10 days; (2) 5 µm histological sectioning and staining with H&E on recovering wound regions, one sample daily for 10 days. More samples were taken from the controls' middle tissues and tissue edges (red and black marks, respectively, in the figure); (3) Immunohistochemical analyses utilizing anti pH3 and Piwi antibodies on 5 µm tissue sections; (4) qPCR analysis on RNA from the controls' middle tissues and edges (red-striped region and green-striped region, respectively), regenerating tissues at 10 h post injury, and fully regenerated tissues. H & E—haematoxylin and eosin.

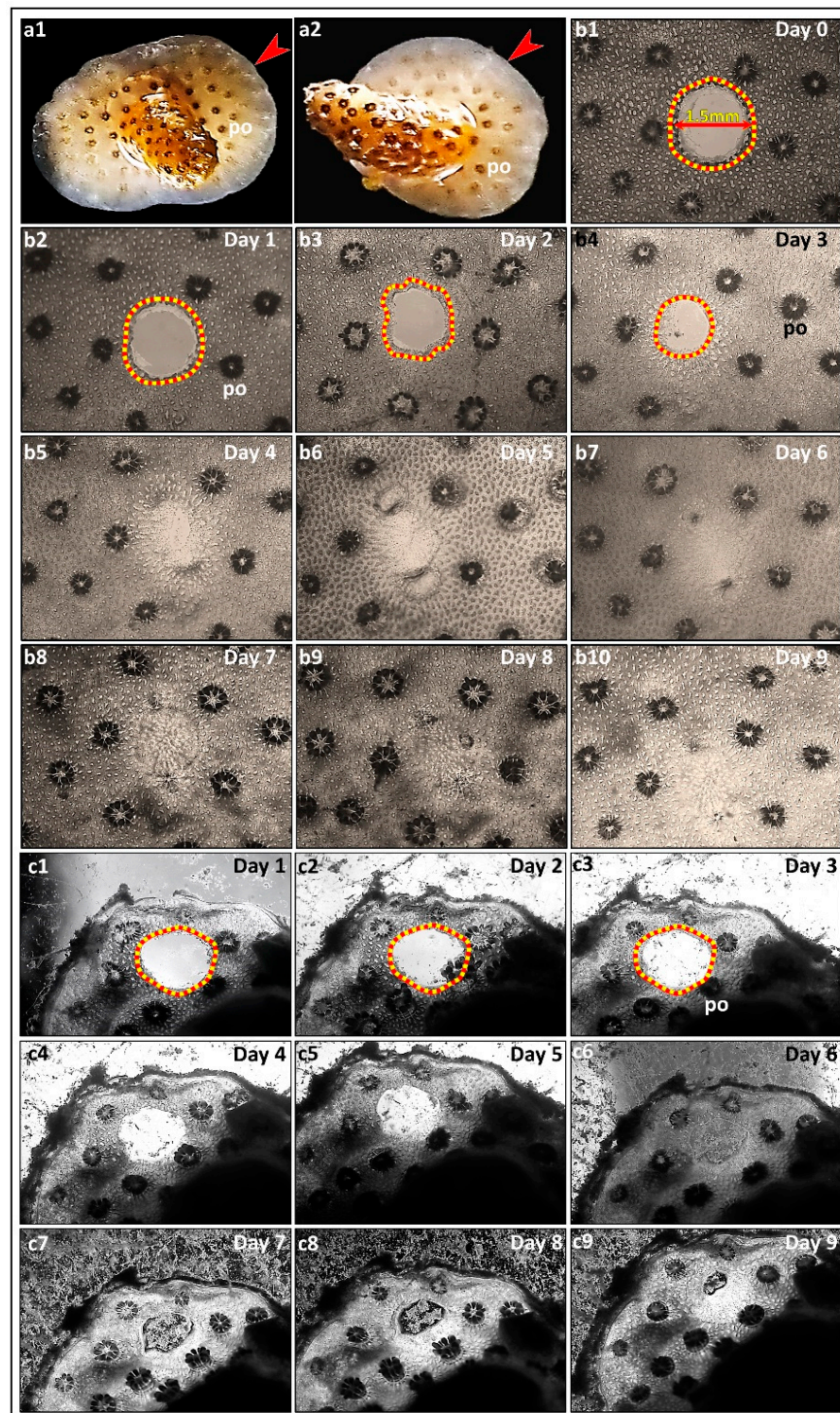


Figure 2. *Stylophora pistillata* regenerating nubbins. (a1,a2) Two *S. pistillata* nubbins with grown and 2D-spread tissue and skeleton over the glass slide ensuing about 70 days of growth following fragmentation (margins indicated by red arrowheads). (b1–b10, c1–c9) Daily images of wound areas in two regeneration assays followed up to 9 days from onset. Both wounds were circular, each 1.5 mm in diameter. (b1–b10) Fully regenerated case by day 6; (c1–c9) partial regeneration. Algal growth in the wound area. Yellow/red dashed lines indicate the wound’s edge. Note the “pale” contour of the regenerated tissue, representing a fewer number of algae. Abbreviation: po—polyp.

2.3. Regeneration Assays

Thirty-four nubbins of each colony were allocated to separate aquaria under similar conditions (one for each colony) for the morphological assay. Regeneration assays (through circular injuries, Figure 1) were performed on the 2D-flattened coral tissues/skeletons on the substrates by punching holes through the tissues and skeletons using a 1.5 mm diameter dermal punch, a procedure which resulted in the complete removal of the entire single polyp. Then, the nubbins were placed back into the aquaria, and each was photographed once a day using a dissection microscope (Nikon SMZ1000, Tokyo, Japan) and a microscope mounted camera (DeltaPix Invenio 3S 11, Smorum, Denmark). Size calibration was performed by photographing a scale attached to a similar glass slide before every daily photographing session. Daily photographing ceased when all injuries either completely healed or stopped regenerating altogether. For each time point, the injury size (surface area) was calculated using the ImageJ 1.52a software. The regeneration rates were calculated on fully regenerating cases. For each genotype, the average area of completely regrown nubbins was divided by the number of days until full regeneration. The Kruskal–Wallis test was used to compare the regeneration rates among the three genotypes, as results did not show a normal distribution. Newly established polyps within the regenerating area or surrounding the injuries were indicated. Two chi-square tests were performed in order to evaluate the emerged number of polyps along full tissue regeneration, the frequency of no-polyps status compared to one-or-more polyps per regenerated site ($n = 64$), and the frequency of a single regenerated polyp compared to two or more polyps ($n = 26$).

2.4. Histology

Ten regenerating nubbins from colony 1 were used for the histological and immunohistochemical assays (Figure 1). One nubbin was sacrificed (by fixation) starting at the injuring time and every 24 h until day 9. Fixation was performed using Bouin's fixative (15:5:1; picric acid, formalin, and acetic acid, respectively) for 2 h and rinsed three times in PBS X3 (three-times-concentrated phosphate-buffered saline) for ten minutes each. One intact nubbin served as the control. The skeletons were decalcified following ref. [55] by submerging them in tri-sodium citrate and slowly dripping formic acid over the nubbin until reaching a ratio of 1:1 and full dissolving of the skeleton. The sectioning protocol followed ref. [56]. Only sections corresponding to the injury area were kept and used going forward. Five slides from each time point ($n = 50$) were stained using a haematoxylin and eosin stain [56]. The stained sections were analysed and photographed using a microscope camera (Nikon DS-Fi2, Tokyo, Japan) coupled with an upright light microscope (Nikon Eclipse Ni-U, Tokyo, Japan) on a DIC mode.

2.5. Immunohistochemistry—Phosphorylated Histone H3, Piwi

Twelve random slides (five per each antibody pH3 [phosphorylated histone H3] and Piwi and one negative control for each antibody) from each time slot ($n = 10$) were used. The slides were washed in xylene twice for ten minutes, then transferred to a decreasing series of ethanol in tris-buffer saline (TBS) (100, 100, 96, 70, 50%), ten minutes in each solution. Later, the slides were microwaved (at 460 W) for 30 min in a Tris-EDTA buffer (600 mL, pH 9), the vessel was topped-up to 1 litre and left to cool down for ten minutes. The slides were washed in TBS and then blocked by incubation in 1% BSA (bovine serum albumin) in TBS for 2 h. Antibodies were applied in 1% BSA-TBS and 0.05% Tween-20 overnight at room temperature. The following antibodies were used: mouse anti-phosphorylated histone H3 monoclonals (1:50, Santa Cruz sc-374669; highly specific, see Supplementary Materials S1) and rabbit anti-*Botrylloides leachii* (Bl)-Piwi polyclonals (1:3000, obtained from [56]. Checked specificity: see Supplementary Materials S2, and Figure S1). Later, the slides were washed five times with TBS, and secondary antibodies were applied to the slides for 2 h at room temperature. The following secondary antibodies were used: Jackson Laboratories goat anti-mouse (1:300, 115-605-003) and goat anti-rabbit (1:300, 111-605-003) Alexa-647. The slides were washed four times in TBS, and DAPI (1 $\mu\text{g}/\text{mL}$) was applied over the slides

for three minutes and then washed once again in TBS. Cover slips were mounted atop the slide using Fluoromount (Sigma-Aldrich, St. Louis, MO, USA).

The stained sections were photographed and analysed using a microscope camera (Nikon DS-Fi2, Tokyo, Japan) coupled with an upright light microscope (Nikon Eclipse Ni-U, Tokyo, Japan) on either a Cy5 (Alexa-647) or a DAPI mode. For each slide, the location and morphology of the stained cells in close vicinity to the wound and regenerating edge were followed.

2.6. Quantitative PCR

Forty-five *S. pistillata* nubbins, fifteen from each of the three colonies, were allocated to a continuously running seawater 20 L tank and were subjected to regeneration assays. Five control tissue samples, designated as RS (resting state), were pooled into a single tube for each genotype. The pooled samples were then fixed in an RLT buffer (supplied with the RNeasy kit; QIAGEN, Hilden, Germany) and stored at -70°C . Tissue samples around the regenerating areas were collected and pooled for groups of five nubbins using 3 mm dermal punches 10 h post injury (assigned as 10 hpi), and five additional samples were taken when the injuries were fully healed (assigned as FH). Additional samples were collected using a scalpel from the peripheries of the laterally grown tissue's edges of five control nubbins and assigned as tissue edges (TE).

Eight genes (*Piwi-1*, *Nanos-1*, *Nanos-1like*, *Tudor-5*, *Tudor-7*, *Boule*, *Sox-2*, and *Myc-1*) were chosen for the comparison of their expression in the four states, and two genes (EIF4A1 and 18S) were used as the normalizing genes in the assay; please refer to Supplementary Table S1. The tested genes were chosen out of <https://www.ncbi.nlm.nih.gov/genbank/> (accessed on 10 February 2024) for being well-established stemness markers used in many similar studies with various animals of the cnidarian phylum.

Total RNA was extracted using RNeasy Mini Kit Cat. No. 74104 and RNase-free DNase kit Cat. No. 79254 (Qiagen, Germany) according to the manufacturer's instructions. First-strand cDNA was synthesized using RevertAid, First Strand cDNA Synthesis Kit cat no. K1622 (Thermo Scientific, Waltham, MA, USA, <https://www.thermofisher.com/il/en/home.html>, accessed on 10 February 2024) according to the manufacturer's instructions.

qPCR analyses were performed with Fast SYBRTM Green Master Mix (cat.no 4385614; Thermo Fisher Scientific, Waltham, MA, USA) according to the manufacturer's instructions using a StepOnePlus Real-Time PCR System (Thermo Fisher Scientific, Waltham, MA, USA). The $\Delta\Delta C_T$ method was used to analyse the relative (fold) changes in the tested genes' expressions in the treated tissues as described by [57]. Statistical analyses were carried out using IBM SPSS 25.0 on three biological replicates. Statistical analyses were carried out on the calculated ΔC_T s using the IBM SPSS 25.0 software on three biological replicates. ΔC_T is the difference between the C_T (threshold cycle) of the examined gene and the average C_T of the normalizing genes (18S and eukaryotic initiation factor 4A-I-like EIF4A1). The analyses were carried out by performing repeated-measures ANOVA and LSD (Fisher's least significant difference) post hoc to compare between the four different biological states described above (RS, 10 hpi, FH, and TE). When data sphericity could not be assumed using Mauchly's test of sphericity, Huynh-Feldt correction was used to determine the significance of the repeated-measures ANOVA.

3. Results

3.1. Morphological Outcomes

All the assays were performed using nubbins that had shown sufficient tissue coverage over the glass slides (Figure 2a1,a2). For each assay, wound healing and regeneration processes were followed up to 9 days post injury (dpi), where most lesions were fully regenerated (Figure 2b1–b10; Table 1). Within this time period, tissue regrew into the wounded tissue-deprived site, where an active polyp resided. In most cases the tissue grew in a nearly symmetrical manner from the circular wounded edges towards the wound's centre. Out of the 75 assays studied for a period of 9 days, in 11 (15.5%; Table 1) the wounds

were not fully regenerated ($\chi^2 (1, N = 75) = 37.45, p < 0.001$). The major cause for incomplete regeneration was algal growth within the wound site (Figure 2c1–c9). The percentages of fully regenerating nubbins per colony varied between 73.3% and 96.3% (Table 1), and it was, on average, 84.5%.

Table 1. The distribution of fully regenerating assays (at 9 days post injury) in the three studied *S. pistillata* genotypes.

Source Colon	Assays (n)	Regeneration Not Completed (n)	Regeneration Completed n	Regeneration Completed %
1	18	2	16	88.89
2	27	1	26	96.29
3	30	8	22	73.33
total	75	11	64	84.51

When complete (100%) coverage of the regenerated areas was achieved, it always occurred on day 9 post injury (Figure 3a), irrespective of the coral genotype. Differences in the genotypes' regeneration rates were noted, yet all three curves showed non-linear growth with similar trajectories. The regeneration rates were calculated for each genotype separately (Figure 3b). The regeneration rate of genotype 2 was significantly higher than genotypes 1 and 3, which were similar (Kruskal–Wallis H test: $X_{22} = 13.359, p = 0.001$).

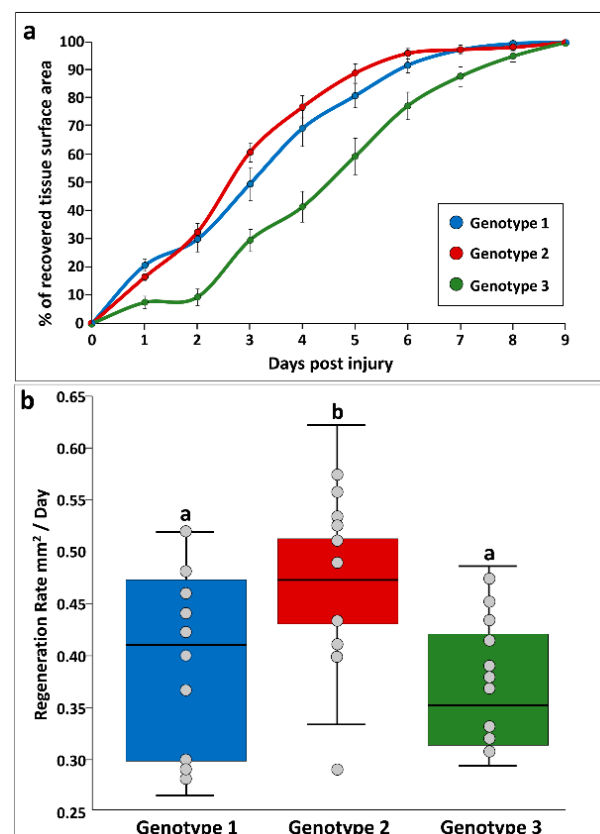


Figure 3. Differences between the three source colonies along the tissue regeneration process following a circular injury. (a) Percentage (\pm SE) of regenerated surface area along nine days from initiation; (b) regeneration rates for the fully regenerated injuries in each genotype. Incompletely healed wounds after a 9-day period were excluded. A comparison among genotypes was conducted using the Kruskal–Wallis H test ($X_{22} = 13.359, p = 0.001$). Similar letters marked on top of the columns indicate non-significant differences.

In every regeneration assay, a single whole polyp was removed for each injury. Yet, by day 9 and at the end of the regeneration process, there were 38 instances where no new polyp had re-appeared (Figure 4a, Table 2), while, in the remaining 26 cases, 1–3 silhouettes of new polyps emerged in close vicinity to the closed wound (Figure 4b–d, Table 2). In order to evaluate the significance of the results (Table 2), two χ^2 tests were performed: (1) a comparison of the options “no polyps” vs. “yes polyps” (38/64 vs. 26/64), χ^2 (1, N = 64) = 2.25, p = 0.13, indicated no significant difference between the options; (2) a comparison of one polyp vs. two or more polyps (22/26 vs. 4/26), χ^2 (1, N = 26) = 12.46, p = 0.00042, showed a significant difference between the two groups, suggesting that, if polyps had formed, there was a significant chance of having only one polyp. This observation potentially challenges the typical pattern formation of polyps’ arrangement seen in *S. pistillata* [17].

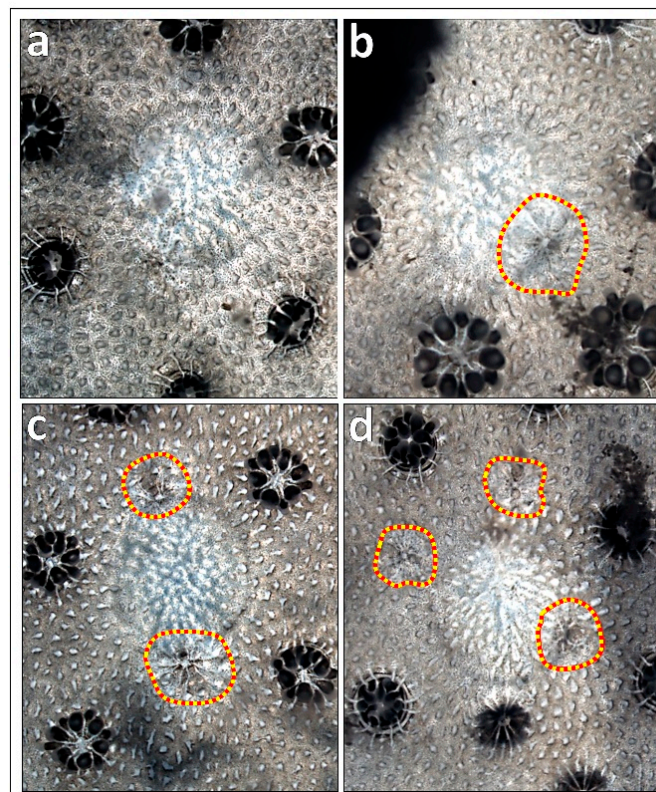


Figure 4. Fully regenerated tissue of *S. pistillata* at 9 days post injury. (a) No polyp regrown in the regenerating wound site, (b–d) silhouettes of 1–3 new polyps in proximity to the regenerating sites (yellow–red-dashed circles).

Table 2. Distribution of the number of polyps formed by 9 dpi (fully tissue regenerated only) for each source colony.

Number of Polyps \ Source Colony	1	2	3	Total
0	13	9	16	38
1	3	13	6	22
2	0	3	0	3
3	0	1	0	1
Total	16	26	22	64

3.2. Histological Observations

The 2D-flattened tissue in our study is composed of polyps interconnected by coenenchyme (Figure 5a). Cross-sections taken at the undamaged coenenchyme (Figure 5b)

display two epithelial layers (epidermis and gastrodermis) and the mesoglea, the interconnecting tissue which links them. Notably, there is a greater presence of zooxanthella in the upper gastrodermal layer compared to the basal (lower) gastrodermis [53]. Due to the aggressive acidic procedure for the skeleton removal and tissue sectioning procedures, the calicoblastic epithelia are barely discernible and appear as some scattered cells located at the lowermost region of the tissue sections.

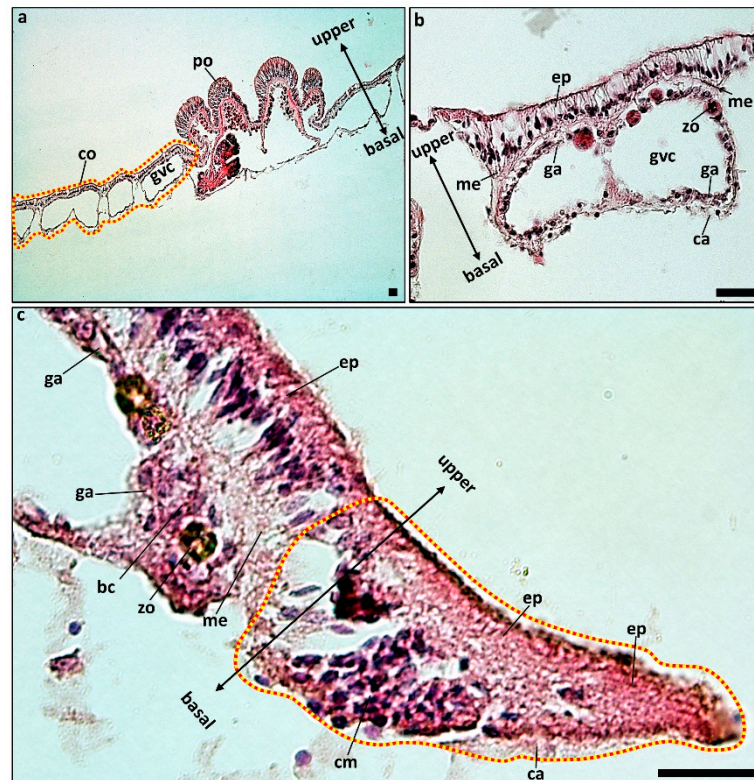


Figure 5. *Stylophora pistillata* cross-sections of normal 2D-flattened tissues stained with haematoxylin and eosin. (a) General structure of the tissue composed of polyps interconnected by the coenenchyme tissue (yellow–red dash-lined area), (b) detailed histological structure of the coenenchyme, and (c) high magnification of the tissue spreading edges. The “addendum”, an expansion of the epidermis, is marked by a yellow–red dashed line. A densely packed cluster of small nuclei (cm) is detected at the aboral side of the “addendum”, a cell organization structure which is not detected anywhere else in the coral tissue. Abbreviations: bc—thick basal gastrodermis; ca—calicoblast; cm—ASCs-like cells; co—coenenchyme; ep—epidermis; ga—gastrodermis; gvc—gastrovascular canals; me—mesoglea; po—polyp; and zo—zooxanthellae. Bar = 20 μ M.

Further, we documented, in the advanced front edges of the nubbins’ 2D-flattened tissues (“addendum”, Figure 5c), dense clusters of nuclei located within the epidermis (“cm” in Figure 5c). This addendum is initiated by the basal calicoblastic layer outward and continues to stretch over the aboral colonial area. A thick mesoglea layer separates the gastrodermis from the epidermis. Within this region, the gastrodermal epithelial cells exhibit increased thickness and robustness, measuring nearly 10 μ m in diameter (“bc” in Figure 5c), gradually becoming thinner, about 5 μ m in more proximal areas. Zooxanthellae are observed in the gastrodermis, positioned quite close to its edge.

Injury is inflicted in such a way that an entire polyp is excised from the tissue. Immediately following the injury, there is a distinct break in the tissue’s continuity (indicated by red scissors), disconnecting opposing tissue sides where the two gastrodermal layers are exposed to the external environment (Figure 6a). During the initial two days following the injury (1–2 dpi, Figure 6b), the tissue fronts of the wound appear to be “sealed” along the injury plan. This sealing is likely a result of the gliding or folding of the exposed upper

epithelial layers. It leads to the formation of an epithelial epidermis that folds over the wound’s margins, connecting both the upper epidermal layer and the basal calcicoblastic layer (connection point indicated with an asterisk, Figure 6b). While intact tissues adjacent to the wound site feature columnar epidermal cells overlying the gastrodermis layer, in the healing tissues, the epidermal epithelium is replaced by an irregular mass of cells that deviates from the typical single-layer columnar cells’ arrangement observed in the epidermis (Figure 6b).

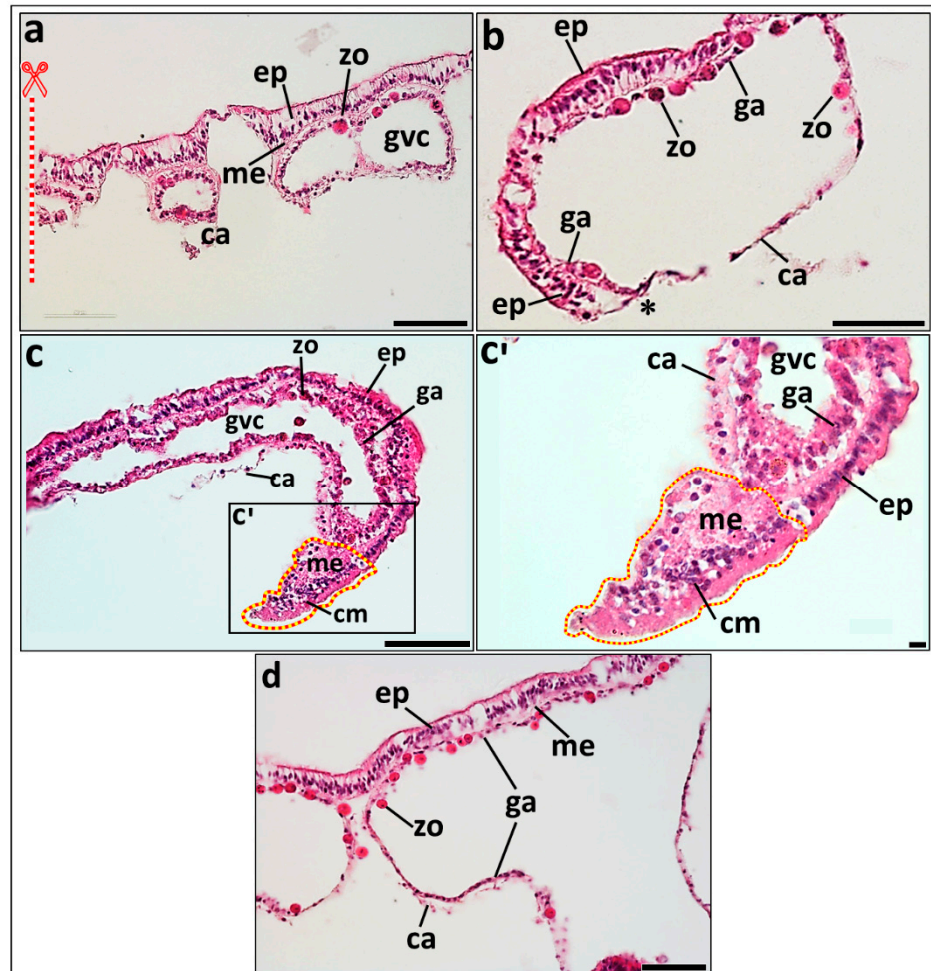


Figure 6. *Stylophora pistillata* cross-sections at the injury site stained with haematoxylin and eosin. (a) Newly injured tissue (0 dpi), bar = 50 μ M; (b) tissue regrowing into the injury site at day 2 (2 dpi), bar = 50 μ M; (c) tissue regrowing into the injury site at day 4 (4 dpi), featuring epidermal epithelium expansion, bar = 100 μ M; (c') zoomed-in figure of the addendum region in the tissue shown in (c), bar = 10 μ M; and (d) fully regenerated tissue at 6 dpi, bar = 50 μ M. Abbreviations: ca—calcicoblast; cm—ASCs-like; ep—epidermis; ga—gastrodermis; gvc—gastrovascular canals; me—mesoglea; and zo—zooxanthellae. An asterisk marks the connecting point of the upper epidermal layer and the basal calcicoblastic layer; scissors mark the injury site. The “addendum” is outlined by a yellow–red-dashed line.

As tissue regeneration advances beyond the initial stages (from 3 dpi onward, achieving complete regeneration), all regenerating assays display the appearance of novel morphological extensions (each called addendum) along the leading edges of the epidermal epithelium. Both the upper and basal boundaries of these extensions (Figure 6c,c') consist of epidermal epithelium. Within the addenda, we frequently note densely packed clusters of small cells (“cm” in Figure 6c,c'). Limited numbers of other cells are dispersed within these extensions, but they are not characterized. The epidermal epithelium expansions

are extended up to about 150 μm , possessing high numbers of seemingly undifferentiated cells, circular in shape and about 5 μm across, resembling earlier observations by [51]. The calicoblastic layer becomes evident just close to the expansion of the epidermal epithelium (Figure 6c,c'). The newly formed gastrodermal epithelium has undergone further development, featuring the presence of intersecting canals within the gastrovascular system, closely resembling the characteristics of typical coral tissues. This also includes the presence of symbiotic algae and densely arranged cells. At the extreme front of the gastrodermis, nearest to the epidermal epithelium's expansion, larger gastrodermal epithelial cells can be observed, measuring nearly 10 μm in diameter and having a more rounded shape, similar to the bc cells marked in Figure 5c. The algae residing in the gastrodermal regions are found in lower densities in this state. In most sections, they appear only 150–200 μm away from the wound site.

Upon achieving complete tissue regeneration (Figure 6d), the majority of epidermal cells have reverted to their single-layer arrangement. The gastrodermis is also fully developed, with a predominant presence of zooxanthellae, mostly within the upper gastrodermis, although some might be found within the basal gastrodermis.

The results reveal a distinct similarity between the initial phases of wound healing and the nubbins' 2D-flattened tissue edges. Dense clusters of cells, presumed to be adult stem cells, are recorded in both developmental phases. These stem-like cells seem to originate from the epidermal tissues, although it remains uncertain whether they permanently reside within this tissue.

3.3. Immunohistochemistry

3.3.1. Phospho-Histone H3 Labelling

Right after the injury, there were randomly dispersed pH3⁺ cells that were roughly evenly distributed within the gastrodermal and epidermal epithelial layers (Figure 7a). No distinct clusters or aggregations of pH3⁺ cells were seen. As expected, the boundaries of the wounds were not highlighted with pH3⁺ cells. At later stages and throughout the entire process of regeneration, a substantial number of pH3⁺ cells was seen at the edges of the injury sites (where active regeneration took place; Figure 7b,c). These cells were particularly concentrated at the very edge, approximately 100–150 μm from the epidermal layer (Figure 7b,c), while only few pH3⁺ cells appeared at the very edge of the gastrodermal layer. The staining was nuclear and differed from the large whole-cell autofluorescence emitted by the zooxanthellae, also seen in the controls reacted with pre-immunized serum (Figure 7b1). Figure 7d,d1 represent the same tissue stained simultaneously with pH3 (Figure 7d) and DAPI (Figure 7d1), revealing that pH3 simultaneously stains nuclei with DAPI, further implying that pH3 is nuclear-specific, as expected. The large red spots indicated by green arrowheads represent a presumable epibiont (Figure 7d).

Similarly, in the healthy epidermal layer lining the spreading edges of the tissue, there was also a notable mass of pH3⁺ cells (Figure 7e). This mass contained a few dozen of distinctly stained cells. Additionally, scattered cells that appeared to be pH3⁺ cells were occasionally observed in the gastrodermis, sometimes gathering together.

3.3.2. PIWI Labelling

Immediately following injuring (Figure 8a,a1), scattered Piwi⁺ cells were seen along all the tissue layers. No specific clusters or aggregations of these cells were observed at this stage, although many stained cells appeared within the polyp's tissues, primarily within its tentacles. The Piwi protein was distinctly stained in the cells' cytoplasm, rather than in their nuclei, as suggested by [58]. Along the regeneration process and tissue rebuilding (Figure 8b,c; 2 and 5 dpi), a significant aggregate of Piwi⁺ cells was visualised as red staining appearing within the cell's cytoplasm, at the foremost region of the expanded epidermal epithelium (Figure 8c,d, 5 dpi), correlating with the H&E staining outcomes for masses of small nuclei observed using H&E staining (Figure 6c) and pH3⁺ cells (Figure 7b–d).

Staining was observed solely in the epidermis. Most of the stained cells were located in the basal epidermis, in close proximity to the newly forming calicoblastic layer.

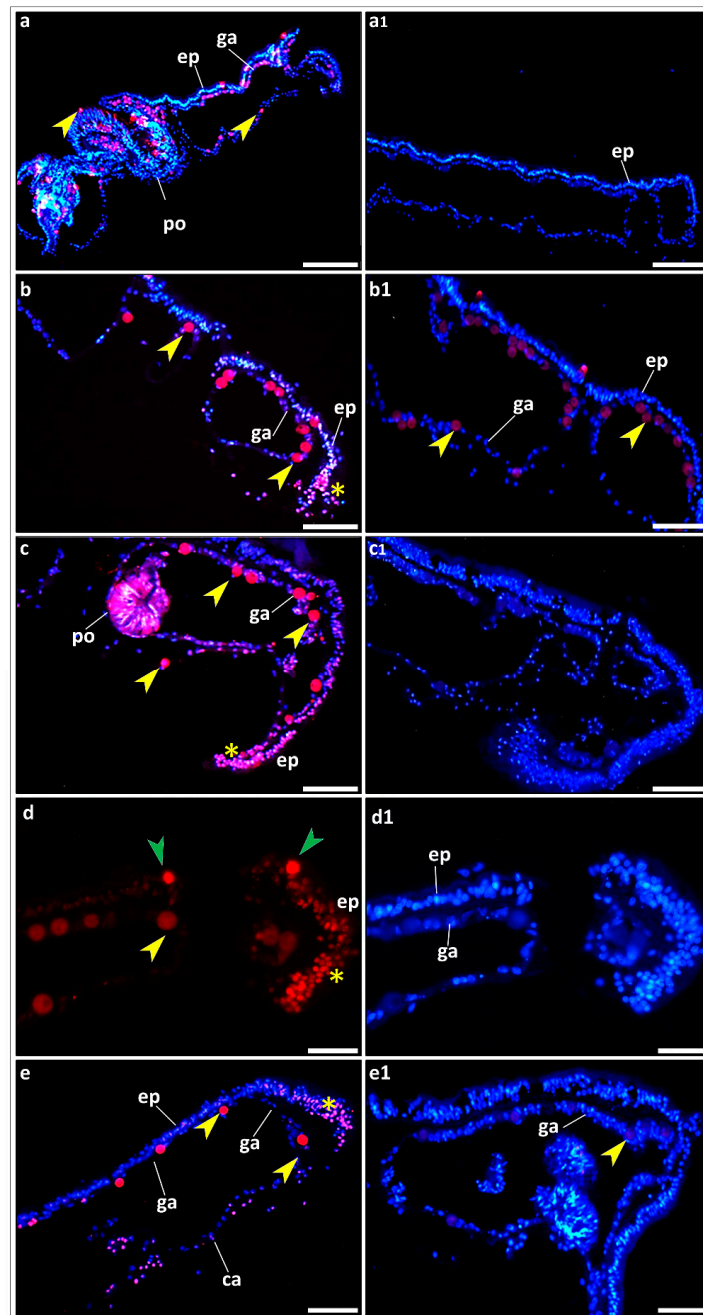


Figure 7. *Stylophora pistillata* cross-sections at the injury site ((a–d, a1–d1)) or at the normal-spreading tissue edge (e,e1) stained with anti-phosphohistone H3 (pH3⁺) antibodies (red) and DAPI (blue). (a,a1) Newly injured tissue (0 dpi); (b,b1) tissue regrowing into the injury site at day 2 (2 dpi); (c,c1) tissue regrowing into the injury site at day 5 (5 dpi), featuring epidermal epithelium expansion; (d,d1) tissue regrowing into the injury site at day 4 (4 dpi); and (e,e1) a spreading nubbin tissue edge. (a1–c1,e1) are the controls, at the same respective dpi (a–c,e), stained with pre-immune serum and DAPI. The tissue in (d) shows fluorescence under the cy5 channel, and the control (d1) image of the same tissue can be seen under the DAPI channel. (a,a1) Scale bars = 100 μm; (b,c,e,b1,c1,e1) scale bars = 50 μm; and (d,d1) scale bars = 25 μm. Nonspecific staining: yellow arrowheads depict zooxanthellae autofluorescence; green arrowheads depict epibiont autofluorescence. Abbreviations: ca—calicoblast; ep—epidermis; ga—gastrodermis; and po—polyp. Asterisks indicate aggregates of pH3⁺ cells.

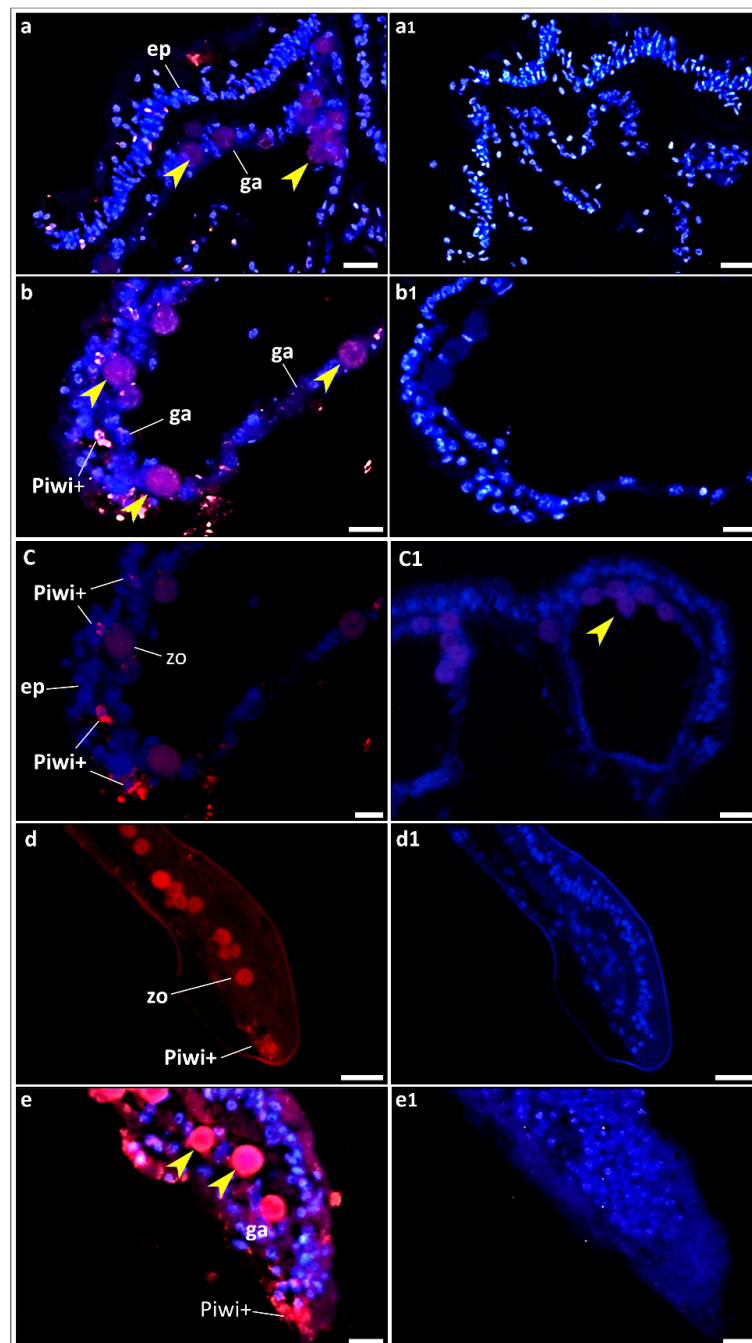


Figure 8. *Stylophora pistillata* cross-sections at the injury site (a–d, a1–d1) and at the normal-spreading tissue edge (e,e1), stained with anti-Piwi antibodies (red) and DAPI (blue). (a,a1) Newly injured tissue (0 dpi); (b,b1) tissue regrowing into the injury site at day 2 (2 dpi); (c,c1) tissue regrowing into the injury site at day 5 (5 dpi), featuring epidermal epithelium expansion; (d,d1) tissue regrowing into the injury site at day 5 (5 dpi); and (e,e1) a spreading nubbin tissue edge. (a1–c1,e1) are the controls, at the same respective dpi (as (a–c,e), respectively), stained with pre-immune serum and DAPI. The tissue in (d) shows fluorescence under the cy5 channel, and the control (d1) image of the same tissue can be seen under the DAPI channel. (a,a1,d,d1) Bar = 20 μ m; and (b,c,e,b1,c1,e1) bar = 10 μ m. Abbreviations: ep—epidermis; ga—gastrodermis; and zo—zooxanthellae. Arrowheads indicate the nonspecific autofluorescence of the zooxanthellae.

In the edge tissues of the spreading 2D-flattened tissue (Figure 8e,e1), an aggregate of Piwi+ cells was observed at the very edge of the expansion of the epidermal epithelium, similar to the aggregate detected in the healing tissue. Another mass of Piwi+ cells was

observed, located approximately 100 μm away from the previously mentioned cluster, at the basal epidermis; yet, they did not exhibit the characteristics of flat calicoblastic cells.

Based on the histological haematoxylin–eosin staining as well as the immunobiological staining (anti-pH3 and anti-Piwi antibodies), a general model elucidating the cellular and molecular mechanisms underlying normal growth in the 2D-flattened tissue of the nubbins and tissue regeneration is presented in Figure 9.

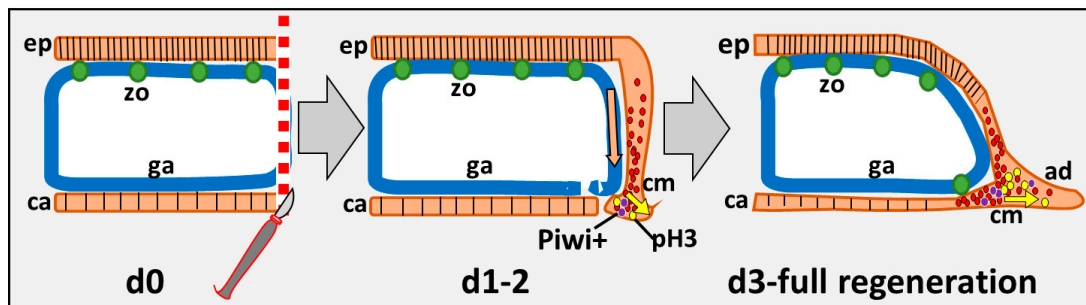


Figure 9. A schematic illustration outlining the proposed mechanism for regenerating coral tissues. d0: a general depiction of the 2D-flattened coral tissue immediately after the infliction of the wound; d1–2: Tissue healing on days 1 and 2 post injury. The upper epidermis glides over the damaged area, folding upon contact with the substrate. It connects with the basal epithelium layer, sealing the wound. A similar movement occurs in the gastrodermis layer. ASCs-like cells migrate within the epithelial tissue towards the substrate, and a new “addendum” structure forms at the joint point between the upper epidermis and the substrate. Piwi+ and pH3+ cells appear. d3—full regeneration: abundant ASCs-like cluster of cells within the “addendum”, with increased stained pH3+ and Piwi+ cell numbers. Abbreviations: ad—addendum; ca—calicoblast; ep—epidermis; ga—gastrodermis; and zo—zooxanthellae. Red dots depict ASCs-like cells, violet dots depict Piwi+ cells, and yellow dots depict pH3+ cells. Yellow arrows indicate the direction of the regenerating front, and the orange arrow shows the direction of movement of the gastrodermis.

3.4. qPCR Analyses

Preliminary experiments established the EIF4A1 and 18S markers as the two best reference genes, representing the least variations and the highest expression stability. The mRNA expressions of the six of the tested genes in our study (*Nanos-1 like*, *Piwi-1*, *Boule*, *Sox-2*, *Tudor-5*, and *Tudor-7*) showed statistically significant changes between the four distinct biological states (Figure 10; Supplementary Tables S2 and S3). The most prominent expression changes were of the *Piwi-1* genes orthologues (accession number: XM_022950268.1) relative to the resting state (naïve state), whose expressions were upregulated between 123-fold in the Reg state (10 h following injury) and 798-fold in the FR (fully regenerated) state. The expression of this *Piwi-1* orthologue was 631 times higher in the spreading tissue edge (TE) when compared with the naïve unhurt tissue. The alterations in the expression of the remaining genes were relatively modest in comparison. The most noteworthy and statistically significant changes were observed in the *Boule*, *Tudor-5*, and *Nanos-1-like* orthologues, which exhibited differences between the naïve tissue and each of the tested treatments. For the *Nanos-1* and *Myc-1* orthologues, a diminution in gene expression was detected at 10 hpi following injury (3.7- and 6-fold decrease, respectively), followed by a non-significant increase in expression in the FR tissue and TE. In summary, there is a consistent pattern of increased gene expression observed across six of the eight genes tested in our study throughout the tissue regeneration process and in the regenerating tissues.

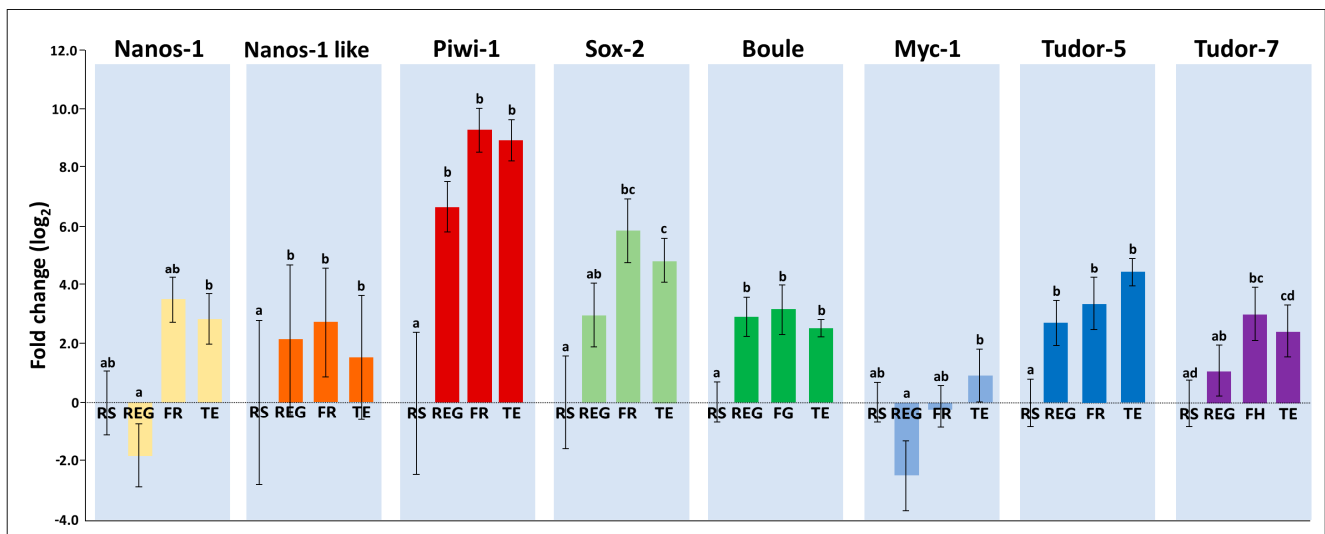


Figure 10. Relative qPCR analyses for eight stemness genes and transcription factors. Tissues from three biological states were sampled: naïve/unhurt tissue (RS (resting state), Reg (10 h post injury), and FR (fully regenerated). Tissues were also sampled from the growing tissue edge (TE) of the intact nubbins. The results are represented as the mean (\pm s.e) of the fold change relative to the RS state, at a log₂ scale. Statistical analyses were performed by repeated-measures ANOVA and LSD (Fisher’s least significant difference) post hoc. Supplementary Table S2 shows the significance values obtained following the repeated-measures ANOVA test. Significant differences following the post hoc tests are shown in Supplementary Table S3. Groups with similar lowercase letters are not significantly different, while those with different letters show statistical significance.

4. Discussion

This study followed the process of tissue regeneration in small circular lesions inflicted upon nubbins of the coral *S. pistillata*, while examining it at the morphological, cellular, and gene expression levels. Remarkably, within just 9 days, 84.5% of the nubbins had fully completed their regeneration, with genotype-specific rates and yet typified by the *S. pistillata*-specific quadratic regression curve. As wound regeneration progressed, a noteworthy development was the emergence of a novel and distinct epidermal epithelium expansion front (“addendum”), spanning approximately 150 μ m. This expansion contained clusters of seemingly undifferentiated cells characterized by small nuclei and expressing well-established markers of proliferation, such as pH3, and the stemness gene marker Piwi. Upon the complete restoration of all epithelial layers, the histology of the normal tissue was reinstated. The cellular and molecular mechanisms governing regeneration closely mimicked the typical growth observed at the coral’s 2D-flattened tissue edges. This involved the development of addendum-like epithelium expansions containing substantial masses of apparently undifferentiated cells and the expression of pH3 and Piwi at the advancing front of the addendum. Along the tissue regeneration and growth processes, changes in the expression of eight genes and transcription factors, correlated with stemness, were observed. In all cases, the spreading nubbin tissue showed an increase in the expression of those eight genes.

The injuries reflected the removal of a single polyp from each nubbin. According to the astogeny rules outlined in [17], it was expected that a single new polyp would re-appear in the centre of the wound site where a polyp had previously existed. However, the results (Figure 4) showed that this expected outcome does not consistently occur. In some cases, no new polyps reappeared, while, in others, 1–3 polyps were reconstructed at the edges of the injuries, thereby breaking the pattern formation morphometric rules established for *S. pistillata*. These rules are believed to be governed by the diffusion of proteins known as morphogens, which inhibit polyp growth, from each polyp to its surrounding tissues. Consequently, a polyp is expected to form in a site where these proteins reach specific

threshold considerations. A possible explanation for the phenomenon of either no polyp formation or the emergence of multiple polyps around the wound site may be related to the impact of tissue cutting on the ability of these compounds to diffuse effectively within the tissue.

This study represents a ground-breaking discovery within the Anthozoa, as it suggests, for the first time, the potential de novo emergence of ASCs-like cells in coral regeneration processes. ASCs have been widely recognized for their involvement in a myriad of biological processes in many studied animals [58–64], particularly in tissue regeneration and growth. In contrast, other cnidarians, such as the well-studied *Hydra* (Hydrozoa), have already revealed the presence of three types of stem cells, that is, ectodermal, endodermal, and interstitial ASCs [36,64]. A recent study [65] further revealed that i-cells in the hydrozoan *Hydractinia* are pluripotent, replacing all the cells of the animal, including its germ cells. Despite belonging to a more basal group [66], which could offer valuable insights into the evolution of ASCs, there is very limited evidence regarding the existence and behaviour of ASCs within the Scleractinia group or any other potential cellular source for tissue growth or regeneration [38,64]. While previous studies have hinted at the presence of i-cells and amoebocytes, a specific niche for these cells as well as their differentiation processes have not been described [48,67,68].

Previous studies, focusing on animals of other taxa, have revealed the formation of blastemal structures at the growth or regeneration fronts [69–72]. These structures typically develop in response to injuries where an animal lost part of one of its organs, following the initial phase of wound healing. Blastemal structures serve as the foundation for regeneration and boast a substantial population of undifferentiated adult stem cells that continuously undergo proliferation to generate a greater number of cells for tissue repair and reorganization [64,70,72–74]. As a result, these blastemal tissues contain a multitude of molecular markers associated with stemness genes and cell proliferation, including Oct-4 and Sox-2 [75], Bruno [76], TRAP [69], Hox [77–79], Ki67 [69], Mps1, and BrdU pulse [80].

In this study, we have revealed the presence of cells expressing genes associated with stem cells and regeneration in both the regenerating and actively growing regions of a scleractinian coral and the potential existence of ASCs-like cells in these tissues. These cells were notably concentrated within the structure of the epidermal epithelium expansion (addendum), which contains a significant population of undifferentiated cells. In addition, the regenerating areas and growing tissue fronts were distinctly marked by the presence of a proliferation marker (pH3) and a stemness marker, Piwi. Furthermore, in the regions at the forefront, encompassing the epidermal expansion, there was a pronounced expression of numerous genes considered as stemness markers (those studied here are *Nanos-1*, *Nanos-1-like Piwi-1*, *Sox-2*, *boule*, *Todur-5*, *Tudor-7*, and *Myc-1*) compared to the unharmed tissue. It is important to note that not all the examined genes were upregulated 10 h post injury (*Nanos-1* and *Myc-1*), yet they did further show non-significant gene upregulation when the injury had fully regenerated. This discrepancy might be attributed to the fact that blastemal formation might not have been established at the earlier time point, resulting in the lack of significant expression of certain stemness markers. The later upregulation of most stemness markers in the fully regenerated tissue suggests the presence of putative ASCs during the tissue rebuilding process.

A recent study [81] suggested the presence of ASCs in the rapidly growing branch tips of *Acropora digitifera* based on the expression pattern of cells that were extracted and cultured from this region. These cultured cells exhibited overexpression of several stemness markers from the *Nanos* gene family previously known from *Hydra*'s i-cells. This finding corresponds with the results presented in our study, suggesting the presence of cells which express stemness markers, along with a proliferation marker, within the blastemal epidermal epithelium expansion in regenerating tissues and tissues spreading over the surface. Yet, another study [82], which compiled an atlas of cells found in *S. pistillata* larvae, primary polyp and adult stony colonies, based on their mRNA expression patterns, did not find any evidence for progenitor or stem cells of any kind. It is noteworthy that the larval

and primary polyp stages feature substantial growth and development. Hence it appears intriguing that indications of stemness are being identified in the growing tissue of mature colonies but not in larvae or juvenile colonies. The characteristics of marine invertebrates' ASCs have been previously discussed [64], revealing that stemness is associated with cellular proliferation and differentiation, further highlighted by specific markers. Yet, the expression of markers alone, without proliferation and differentiation, is not enough to confirm stemness. Thus, only part of the characteristics associated with stemness has been elucidated in the present study. Differentiation of the ASCs-like cells was not directly demonstrated and needs further work.

Our study has, for the first time, provided evidence of the presence and the involvement of ASCs-like cells in the process of tissue regeneration following injuries in the stony coral *S. pistillata*. These cells appear to congregate within an epidermal epithelium expansion, reminiscent of the blastemal structure observed in many animals during their organ regeneration processes. The developing structures and the cells they contain bear similarities to those found at the edges of a spreading coral nubbin over a surface. These findings may contribute to a better understanding of the mechanisms by which scleractinian corals perform tissue regeneration and growth and could potentially bridge the gap towards developing a uniform know-how for tissue renewal across the cnidarian phylum.

Supplementary Materials: The following supporting information can be downloaded at <https://www.mdpi.com/article/10.3390/jmse12020343/s1>: Table S1: Primers used for the qPCR assays; Table S2: Comparison of gene expression among naïve tissues, regenerating tissues, and growing edges: calculated *p*-values by repeated-measures ANOVA analyses; Table S3: *p*-values from LSD (Fisher's least significant difference) post hoc comparisons for significant differences among four biological states; Supplementary S1: Specificity of antibody: p-histone H3 antibody (C-2): sc-374669, Santa Cruz; Supplementary S2: Specificity of antibody: rabbit anti-*Bl*-Piwi polyclonals; Figure S1: Western blot analysis of *Stylophora pistillata* Piwi protein using *Bl*-Piwi.

Author Contributions: Conceptualization, B.R.; methodology, J.L., A.R. and Z.L.; validation, J.L., A.R. and B.R.; analysis, J.L. and A.R.; supervision, B.R.; investigation, J.L. and A.R.; resources, B.R.; data curation, J.L.; writing—original draft preparation, J.L. and B.R.; writing—review and editing, all authors; funding acquisition, B.R. All authors have read and agreed to the published version of the manuscript.

Funding: This research was funded by the ISF (number 3511/21)–NSFC (number 42161144006) Joint Scientific Research Program and by the Ocean Citizen EC-Horizon program no. 101093910 (to B.R.).

Institutional Review Board Statement: Sampling of coral tissues was conducted under a permit from the Israel Ministry of the Environment.

Informed Consent Statement: Not applicable.

Data Availability Statement: Data are contained within the article and Supplementary Materials.

Acknowledgments: We thank E.N. Rachmilovitz and O. (Shabby) Leber-Shabbat for their assistance in collecting the coral colonies and their constant support, I. Kamer for the Western blotting, S. Shafir for their advice, and all the other members of the IOLR marine invertebrate lab.

Conflicts of Interest: The authors declare no conflicts of interest.

References

1. Technau, U.; Steele, R.E. Evolutionary Crossroads in Developmental Biology: Cnidaria. *Development* **2011**, *138*, 1447–1458. [[CrossRef](#)]
2. Fujita, S.; Kuranaga, E.; Nakajima, Y. Regeneration Potential of Jellyfish: Cellular Mechanisms and Molecular Insights. *Genes* **2021**, *12*, 758. [[CrossRef](#)]
3. Henry, L.-A.; Hart, M. Regeneration from Injury and Resource Allocation in Sponges and Corals—a Review. *Int. Rev. Hydrobiol. J. Cover. All Asp. Limnol. Mar. Biol.* **2005**, *90*, 125–158. [[CrossRef](#)]
4. Lirman, D. Lesion Regeneration in the Branching Coral *Acropora palmata*: Effects of Colonization, Colony Size, Lesion Size, and Lesion Shape. *Mar. Ecol. Prog. Ser.* **2000**, *197*, 209–215. [[CrossRef](#)]

5. Meesters, E.H.; Pauchli, W.; Bak, R.P. Predicting Regeneration of Physical Damage on a Reef-Building Coral by Regeneration Capacity and Lesion Shape. *Mar. Ecol. Prog. Ser.* **1997**, *146*, 91–99. [[CrossRef](#)]
6. Luz, B.L.P.; Capel, K.C.C.; Zilberberg, C.; Flores, A.A.V.; Migotto, A.E.; Kitahara, M.V. A Polyp from Nothing: The Extreme Regeneration Capacity of the Atlantic Invasive Sun Corals *Tubastraea coccinea* and *T. tagusensis* (Anthozoa, Scleractinia). *J. Exp. Mar. Biol. Ecol.* **2018**, *503*, 60–65. [[CrossRef](#)]
7. Luz, B.L.P.; Miller, D.J.; Kitahara, M.V. High Regenerative Capacity Is a General Feature within Colonial Dendrophylliid Corals (Anthozoa, Scleractinia). *J. Exp. Zool. Part B Mol. Dev. Evol.* **2021**, *336*, 281–292. [[CrossRef](#)] [[PubMed](#)]
8. Cole, A.J.; Pratchett, M.S.; Jones, G.P. Diversity and Functional Importance of Coral-Feeding Fishes on Tropical Coral Reefs. *Fish Fish.* **2008**, *9*, 286–307. [[CrossRef](#)]
9. Baums, I.B.; Miller, M.W.; Szmant, A.M. Ecology of a Corallivorous Gastropod, *Coralliophila abbreviata*, on Two Scleractinian Hosts. I: Population Structure of Snails and Corals. *Mar. Biol.* **2003**, *142*, 1083–1091. [[CrossRef](#)]
10. Harmelin-Vivien, M.L. The Effects of Storms and Cyclones on Coral Reefs: A Review. *J. Coast. Res.* **1994**, 211–231.
11. Dollar, S.J.; Tribble, G.W. Recurrent Storm Disturbance and Recovery: A Long-Term Study of Coral Communities in Hawaii. *Coral Reefs* **1993**, *12*, 223–233. [[CrossRef](#)]
12. Rogers, C.S.; Gilnack, M.; Fitz III, H.C. Monitoring of Coral Reefs with Linear Transects: A Study of Storm Damage. *J. Exp. Mar. Biol. Ecol.* **1983**, *66*, 285–300. [[CrossRef](#)]
13. Meesters, E.H.; Wesseling, I.; Bak, R.P. Partial Mortality in Three Species of Reef-Building Corals and the Relation with Colony Morphology. *Bull. Mar. Sci.* **1996**, *58*, 838–852.
14. Rinkevich, B. Do Reproduction and Regeneration in Damaged Corals Compete for Energy Allocation? *Mar. Ecol. Prog. Ser.* **1996**, *143*, 297–302. [[CrossRef](#)]
15. Oren, U.; Rinkevich, B.; Loya, Y. Oriented Intra-Colonial Transport of ¹⁴C Labeled Materials during Coral Regeneration. *Mar. Ecol. Prog. Ser.* **1997**, *161*, 117–122. [[CrossRef](#)]
16. Shaish, L.; Abelson, A.; Rinkevich, B. Branch to Colony Trajectory in a Modular Organism: Pattern Formation in the Indo-Pacific Coral *Stylophora pistillata*. *Dev. Dyn.* **2006**, *235*, 2111–2121. [[CrossRef](#)]
17. Guerrini, G.; Shefy, D.; Shashar, N.; Shafir, S.; Rinkevich, B. Morphometric and Allometric Rules of Polyp's Landscape in Regular and Chimeric Coral Colonies of the Branching Species *Stylophora pistillata*. *Dev. Dyn.* **2021**, *250*, 652–668. [[CrossRef](#)]
18. Mullen, K.M.; Peters, E.C.; Harvell, C.D. Coral Resistance to Disease. In *Coral Health and Disease*; Springer: Berlin/Heidelberg, Germany, 2004; pp. 377–399.
19. Rodríguez, S.; Croquer, A.; Guzmán, H.M.; Bastidas, C. A Mechanism of Transmission and Factors Affecting Coral Susceptibility to *Halofolliculina* Sp. Infection. *Coral Reefs* **2009**, *28*, 67–77. [[CrossRef](#)]
20. Voss, J.D.; Richardson, L.L. Nutrient Enrichment Enhances Black Band Disease Progression in Corals. *Coral Reefs* **2006**, *25*, 569–576. [[CrossRef](#)]
21. Diaz-Pulido, G.; McCook, L.J.; Dove, S.; Berkelmans, R.; Roff, G.; Kline, D.I.; Weeks, S.; Evans, R.D.; Williamson, D.H.; Hoegh-Guldberg, O. Doom and Boom on a Resilient Reef: Climate Change, Algal Overgrowth and Coral Recovery. *PLoS ONE* **2009**, *4*, e5239. [[CrossRef](#)] [[PubMed](#)]
22. Child, C.M. Form Regulation in *Cerianthus*: I. The Typical Course of Regeneration. *Biol. Bull.* **1903**, *5*, 239–260. [[CrossRef](#)]
23. Cróquer, A.; Villamizar, E.; Noriega, N. Environmental factors affecting tissue regeneration of the reef-building coral *Montastraea annularis* (Faviidae) at Los Roques National Park, Venezuela. *Rev. Biol. Trop.* **2002**, *50*(3-4), 1055–1065.
24. Hall, V.R. Interspecific Differences in the Regeneration of Artificial Injuries on Scleractinian Corals. *J. Exp. Mar. Biol. Ecol.* **1997**, *212*, 9–23. [[CrossRef](#)]
25. Meesters, E.H.; Noordeloos, M.; Bak, R.P. Damage and Regeneration: Links to Growth in the Reef-Building Coral *Montastrea annularis*. *Mar. Ecol. Prog. Ser.* **1994**, *112*, 119–128. [[CrossRef](#)]
26. Meesters, E.H.; Wesseling, I.; Bak, R.P. Coral Colony Tissue Damage in Six Species of Reef-Building Corals: Partial Mortality in Relation with Depth and Surface Area. *J. Sea Res.* **1997**, *37*, 131–144. [[CrossRef](#)]
27. Meesters, E.H.; Bak, R.P. Effects of Coral Bleaching on Tissue Regeneration Potential and Colony Survival. *Mar. Ecol. Prog. Ser.* **1993**, *96*, 189–198. [[CrossRef](#)]
28. Meesters, E.H.; Bak, R.P. Age-Related Deterioration of a Physiological Function in the Branching Coral *Acropora palmata*. *Mar. Ecol. Prog. Ser.* **1995**, *121*, 203–209. [[CrossRef](#)]
29. Titlyanov, E.A.; Titlyanova, T.V.; Yakovleva, I.M.; Nakano, Y.; Bhagooli, R. Regeneration of Artificial Injuries on Scleractinian Corals and Coral/Algal Competition for Newly Formed Substrate. *J. Exp. Mar. Biol. Ecol.* **2005**, *323*, 27–42. [[CrossRef](#)]
30. Bonesso, J.L.; Leggat, W.; Ainsworth, T.D. Exposure to Elevated Sea-Surface Temperatures below the Bleaching Threshold Impairs Coral Recovery and Regeneration Following Injury. *PeerJ* **2017**, *5*, e3719. [[CrossRef](#)]
31. Counsell, C.W.; Johnston, E.C.; Sale, T.L. Colony Size and Depth Affect Wound Repair in a Branching Coral. *Mar. Biol.* **2019**, *166*, 148. [[CrossRef](#)]
32. Kaufman, M.L.; Watkins, E.; van Hooideonk, R.; Baker, A.C.; Lirman, D. Thermal History Influences Lesion Recovery of the Threatened Caribbean Staghorn Coral *Acropora cervicornis* under Heat Stress. *Coral Reefs* **2021**, *40*, 289–293. [[CrossRef](#)]
33. Horricks, R.A.; Herbinger, C.M.; Lillie, B.N.; Taylor, P.; Lumsden, J.S. Differential Protein Abundance during the First Month of Regeneration of the Caribbean Star Coral *Montastraea cavernosa*. *Coral Reefs* **2019**, *38*, 45–61. [[CrossRef](#)]

34. Horricks, R.A.; Herbing, C.M.; Vickaryous, M.K.; Taylor, P.; Lumsden, J.S. Differential Protein Abundance Associated with Delayed Regeneration of the Scleractinian Coral *Montastraea cavernosa*. *Coral Reefs* **2020**, *39*, 1175–1186. [[CrossRef](#)]
35. Bode, H.R. Head Regeneration in Hydra. *Dev. Dyn. Off. Publ. Am. Assoc. Anat.* **2003**, *226*, 225–236. [[CrossRef](#)] [[PubMed](#)]
36. Bosch, T.C.G. Hydra and the Evolution of Stem Cells. *BioEssays* **2009**, *31*, 478–486. [[CrossRef](#)]
37. Gierer, A.; Berking, S.; Bode, H.; David, C.N.; Flick, K.; Hansmann, G.; Schaller, H.; Trenkner, E. Regeneration of *Hydra* from Reaggregated Cells. *Nat. New Biol.* **1972**, *239*, 98–101. [[CrossRef](#)] [[PubMed](#)]
38. Gold, D.A.; Jacobs, D.K. Stem Cell Dynamics in Cnidaria: Are There Unifying Principles? *Dev. Genes Evol.* **2013**, *223*, 53–66. [[CrossRef](#)] [[PubMed](#)]
39. Vogg, M.C.; Galliot, B.; Tsiairis, C.D. Model Systems for Regeneration: *Hydra*. *Development* **2019**, *146*, dev177212. [[CrossRef](#)]
40. Lesh-Laurie, G.E.; Hujer, A.; Suchy, P. Polyp Regeneration from Isolated Tentacles of *Aurelia scyphistomae*: A Role for Gating Mechanisms and Cell Division. In *Coelenterate Biology: Recent Research on Cnidaria and Ctenophora*; Springer: Berlin/Heidelberg, Germany, 1991; pp. 91–97.
41. Nakanishi, N.; Yuan, D.; Jacobs, D.K.; Hartenstein, V. Early Development, Pattern, and Reorganization of the Planula Nervous System in *Aurelia* (Cnidaria, Scyphozoa). *Dev. Genes Evol.* **2008**, *218*, 511–524. [[CrossRef](#)]
42. Steinberg, S.N. The Regeneration of Whole Polyps from Ectodermal Fragments of Scyphistoma Larvae of *Aurelia aurita*. *Biol. Bull.* **1963**, *124*, 337–343. [[CrossRef](#)]
43. Yuan, D.; Nakanishi, N.; Jacobs, D.K.; Hartenstein, V. Embryonic Development and Metamorphosis of the Scyphozoan *Aurelia*. *Dev. Genes Evol.* **2008**, *218*, 525–539. [[CrossRef](#)] [[PubMed](#)]
44. Hutton, D.M.; Smith, V.J. Antibacterial Properties of Isolated Amoebocytes from the Sea Anemone *Actinia equina*. *Biol. Bull.* **1996**, *191*, 441–451. [[CrossRef](#)] [[PubMed](#)]
45. Meszaros, A.; Bigger, C. Qualitative and Quantitative Study of Wound Healing Processes in the Coelenterate, *Plexaurella fusifera*: Spatial, Temporal, and Environmental (Light Attenuation) Influences. *J. Invertebr. Pathol.* **1999**, *73*, 321–331. [[CrossRef](#)]
46. Mydlarz, L.D.; Holthouse, S.F.; Peters, E.C.; Harvell, C.D. Cellular Responses in Sea Fan Corals: Granular Amoebocytes React to Pathogen and Climate Stressors. *PLoS ONE* **2008**, *3*, e1811. [[CrossRef](#)] [[PubMed](#)]
47. Olano, C.T.; Bigger, C.H. Phagocytic Activities of the Gorgonian Coral *Swiftia exserta*. *J. Invertebr. Pathol.* **2000**, *76*, 176–184. [[CrossRef](#)]
48. Palmer, C.V.; Traylor-Knowles, N.G.; Willis, B.L.; Bythell, J.C. Corals Use Similar Immune Cells and Wound-Healing Processes as Those of Higher Organisms. *PLoS ONE* **2011**, *6*, e23992. [[CrossRef](#)]
49. Patterson, M.J.; Landolt, M.L. Cellular Reaction to Injury in the Anthozoan *Anthopleura elegantissima*. *J. Invertebr. Pathol.* **1979**, *33*, 189–196. [[CrossRef](#)]
50. Vargas-Ángel, B.; Peters, E.C.; Kramarsky-Winter, E.; Gilliam, D.S.; Dodge, R.E. Cellular Reactions to Sedimentation and Temperature Stress in the Caribbean Coral *Montastraea cavernosa*. *J. Invertebr. Pathol.* **2007**, *95*, 140–145. [[CrossRef](#)] [[PubMed](#)]
51. Raz-Bahat, M.; Erez, J.; Rinkevich, B. In Vivo Light-Microscopic Documentation for Primary Calcification Processes in the Hermatypic Coral *Stylophora pistillata*. *Cell Tissue Res.* **2006**, *325*, 361–368. [[CrossRef](#)] [[PubMed](#)]
52. Shefy, D.; Rinkevich, B. *Stylophora pistillata*—A Model Colonial Species in Basic and Applied Studies. In *Handbook of Marine Model Organisms in Experimental Biology—Established and Emerging*; Boutet, A., Schierwater, B., Eds.; CRC Press: Boca Raton, FL, USA, 2021; pp. 195–216.
53. Bockel, T.; Rinkevich, B. Rapid Recruitment of Symbiotic Algae into Developing Scleractinian Coral Tissues. *J. Mar. Sci. Eng.* **2019**, *7*, 306. [[CrossRef](#)]
54. Shafir, S.; Van Rijn, J.; Rinkevich, B. Nubbing of Coral Colonies: A Novel Approach for the Development of Inland Broodstocks. *Aquar. Sci. Conserv.* **2001**, *3*, 183–190. [[CrossRef](#)]
55. Rinkevich, B.; Loya, Y. The Reproduction of the Red Sea Coral *Stylophora Pistillata*. I. Gonads and Planulae. *Mar. Ecol. Prog. Ser.* **1979**, *1*, 133–144. [[CrossRef](#)]
56. Rinkevich, Y.; Rosner, A.; Rabinowitz, C.; Lapidot, Z.; Moiseeva, E.; Rinkevich, B. Piwi Positive Cells That Line the Vasculature Epithelium, Underlie Whole Body Regeneration in a Basal Chordate. *Dev. Biol.* **2010**, *345*, 94–104. [[CrossRef](#)]
57. Pfaffl, M.W. A New Mathematical Model for Relative Quantification in Real-Time RT-PCR. *Nucleic Acids Res.* **2001**, *29*, e45. [[CrossRef](#)]
58. Juliano, C.E.; Reich, A.; Liu, N.; Götzfried, J.; Zhong, M.; Uman, S.; Reenan, R.A.; Wessel, G.M.; Steele, R.E.; Lin, H. PIWI Proteins and PIWI-Interacting RNAs Function in *Hydra* Somatic Stem Cells. *Proc. Natl. Acad. Sci. USA* **2014**, *111*, 337–342. [[CrossRef](#)] [[PubMed](#)]
59. Fierro-Constaín, L.; Schenkelaars, Q.; Gazave, E.; Haguenaer, A.; Rocher, C.; Ereskovsky, A.; Borchiellini, C.; Renard, E. The Conservation of the Germline Multipotency Program, from Sponges to Vertebrates: A Stepping Stone to Understanding the Somatic and Germline Origins. *Genome Biol. Evol.* **2017**, *9*, 474–488. [[CrossRef](#)] [[PubMed](#)]
60. Cervello, I.; Simon, C. Somatic Stem Cells in the Endometrium. *Reprod. Sci.* **2009**, *16*, 200–205. [[CrossRef](#)] [[PubMed](#)]
61. Shibata, N.; Umesono, Y.; Orii, H.; Sakurai, T.; Watanabe, K.; Agata, K. Expression Ofvasa (Vas)-Related Genes in Germline Cells and Totipotent Somatic Stem Cells of Planarians. *Dev. Biol.* **1999**, *206*, 73–87. [[CrossRef](#)] [[PubMed](#)]
62. Shukalyuk, A.I.; Golovkina, K.A.; Baiborodin, S.I.; Gunbin, K.V.; Blinov, A.G.; Isaeva, V.V. Vasa-Related Genes and Their Expression in Stem Cells of Colonial Parasitic Rhizocephalan Barnacle *Polyascus polygena* (Arthropoda: Crustacea: Cirripedia: Rhizocephala). *Cell Biol. Int.* **2007**, *31*, 97–108. [[CrossRef](#)] [[PubMed](#)]

63. Rink, J.C. Stem Cell Systems and Regeneration in Planaria. *Dev. Genes Evol.* **2013**, *223*, 67–84. [[CrossRef](#)] [[PubMed](#)]
64. Rinkevich, B.; Ballarin, L.; Martinez, P.; Somorjai, I.; Ben-Hamo, O.; Borisenko, I.; Berezikov, E.; Ereskovsky, A.; Gazave, E.; Khnykin, D.; et al. A pan-metazoan concept for adult stem cells: The wobbling Penrose landscape. *Biol. Rev.* **2022**, *97*, 299–325. [[CrossRef](#)]
65. Varley, Á.; Horkan, H.R.; McMahon, E.T.; Krasovec, G.; Frank, U. Pluripotent, germ cell competent adult stem cells underlie cnidarian regenerative ability and clonal growth. *Curr. Biol.* **2023**, *33*, 1883–1892. [[CrossRef](#)] [[PubMed](#)]
66. Collins, A. Recent Insights into Cnidarian Phylogeny. *Smithson. Contrib. Mar. Sci.* **2009**, *38*, 140–149.
67. Reyes-Bermudez, A.; Miller, D.J. In Vitro Culture of Cells Derived from Larvae of the Staghorn Coral *Acropora millepora*. *Coral Reefs* **2009**, *28*, 859–864. [[CrossRef](#)]
68. Martinez Serra, P.; Ballarin, L.; Ereskovsky, A.V.; Gazave, E.; Hobmayer, B.; Manni, L.; Rottinger, E.; Sprecher, S.G.; Tiozzo, S.; Varela-Coelho, A.; et al. Articulating the “stem cell niche” paradigm through the lens of non-model aquatic invertebrates. *BMC Biol.* **2022**, *20*, 23. [[CrossRef](#)] [[PubMed](#)]
69. Fernando, W.A.; Leininger, E.; Simkin, J.; Li, N.; Malcom, C.A.; Sathyamoorthi, S.; Han, M.; Muneoka, K. Wound Healing and Blastema Formation in Regenerating Digit Tips of Adult Mice. *Dev. Biol.* **2011**, *350*, 301–310. [[CrossRef](#)] [[PubMed](#)]
70. McCusker, C.; Bryant, S.V.; Gardiner, D.M. The Axolotl Limb Blastema: Cellular and Molecular Mechanisms Driving Blastema Formation and Limb Regeneration in Tetrapods. *Regeneration* **2015**, *2*, 54–71. [[CrossRef](#)]
71. Saló, E.; Baguna, J. Regeneration and Pattern Formation in Planarians. II. and Role of Cell Movements in Blastema Formation. *Development* **1989**, *107*, 69–76. [[CrossRef](#)]
72. Santos-Ruiz, L.; Santamaría, J.A.; Ruiz-Sánchez, J.; Becerra, J. Cell Proliferation during Blastema Formation in the Regenerating Teleost Fin. *Dev. Dyn. Off. Publ. Am. Assoc. Anat.* **2002**, *223*, 262–272. [[CrossRef](#)]
73. Tamura, K.; Ohgo, S.; Yokoyama, H. Limb Blastema Cell: A Stem Cell for Morphological Regeneration. *Dev. Growth Differ.* **2010**, *52*, 89–99. [[CrossRef](#)]
74. Tsonis, P.A. Stem Cells and Blastema Cells. *Curr. Stem Cell Res. Ther.* **2008**, *3*, 53–54. [[CrossRef](#)] [[PubMed](#)]
75. Moghaddam Matin, M.; Saeinasab, M.; Nakhaei-Rad, S.; Mirahmadi, M.; Mahdavi Shahri, N.; Mahmoudi, M.; Bahrami, A.R. Blastema Cells Derived from Rabbit Ear Show Stem Cell Characteristics. *J. Cell Mol. Res.* **2011**, *3*, 25–30.
76. Guo, T.; Peters, A.H.F.M.; Newmark, P.A. A Bruno-like Gene Is Required for Stem Cell Maintenance in Planarians. *Dev. Cell* **2006**, *11*, 159–169. [[CrossRef](#)] [[PubMed](#)]
77. Bayascas, J.R.; Castillo, E.; Salo, E. Platyhelminthes Have a Hox Code Differentially Activated during Regeneration, with Genes Closely Related to Those of Spiralian Protostomes. *Dev. Genes Evol.* **1998**, *208*, 467–473. [[CrossRef](#)]
78. Orii, H.; Kato, K.; Umesono, Y.; Sakurai, T.; Agata, K.; Watanabe, K. The Planarian HOM/HOX Homeobox Genes (Plox) Expressed along the Anteroposterior Axis. *Dev. Biol.* **1999**, *210*, 456–468. [[CrossRef](#)]
79. Nogi, T.; Watanabe, K. Position-Specific and Non-Colinear Expression of the Planarian Posterior (Abdominal-B-like) Gene. *Dev. Growth Differ.* **2001**, *43*, 177–184. [[CrossRef](#)] [[PubMed](#)]
80. Poss, K.D.; Nechiporuk, A.; Hillam, A.M.; Johnson, S.L.; Keating, M.T. Mps1 Defines a Proximal Blastemal Proliferative Compartment Essential for Zebrafish Fin Regeneration. *Development* **2002**, *129*, 5141–5149. [[CrossRef](#)]
81. Reyes-Bermudez, A.; Hidaka, M.; Mikheyev, A. Transcription Profiling of Cultured *Acropora digitifera* Adult Cells Reveals the Existence of Ancestral Genome Regulatory Modules Underlying Pluripotency and Cell Differentiation in Cnidaria. *Genome Biol. Evol.* **2021**, *13*, evab008. [[CrossRef](#)]
82. Levy, S.; Elek, A.; Grau-Bové, X.; Menéndez-Bravo, S.; Iglesias, M.; Tanay, A.; Mass, T.; Sebé-Pedrós, A. A Stony Coral Cell Atlas Illuminates the Molecular and Cellular Basis of Coral Symbiosis, Calcification, and Immunity. *Cell* **2021**, *184*, 2973–2987.e18. [[CrossRef](#)]

Disclaimer/Publisher’s Note: The statements, opinions and data contained in all publications are solely those of the individual author(s) and contributor(s) and not of MDPI and/or the editor(s). MDPI and/or the editor(s) disclaim responsibility for any injury to people or property resulting from any ideas, methods, instructions or products referred to in the content.